



## Status of the HOLMES Experiment

M. De Gerone<sup>1</sup> · B. Alpert<sup>3</sup> · M. Balata<sup>4</sup> · D. T. Becker<sup>3</sup> · D. A. Bennett<sup>3</sup> · A. Bevilacqua<sup>1</sup> · M. Borghesi<sup>5,6</sup> · G. Ceruti<sup>5</sup> · G. De Bodin De Galebent<sup>7</sup> · R. Dressler<sup>7</sup> · M. Faverzani<sup>5,6</sup> · M. Fedkevych<sup>1,2</sup> · E. Ferri<sup>5</sup> · J. W. Fowler<sup>3</sup> · G. Gallucci<sup>1</sup> · J. D. Gard<sup>3</sup> · F. Gatti<sup>1,2</sup> · A. Giachero<sup>5,6</sup> · G. C. Hilton<sup>3</sup> · U. Köster<sup>8</sup> · M. Lusignoli<sup>9</sup> · P. Manfrinetti<sup>10</sup> · J. A. B. Mates<sup>3</sup> · E. Maugeri<sup>7</sup> · S. Nisi<sup>4</sup> · A. Nucciotti<sup>5,6</sup> · L. Parodi<sup>1</sup> · G. Pessina<sup>5,6</sup> · S. Ragazzi<sup>5,6</sup> · C. D. Reintsema<sup>3</sup> · D. R. Schmidt<sup>3</sup> · D. Schumann<sup>7</sup> · F. Siccardi<sup>1</sup> · D. S. Swetz<sup>3</sup> · J. N. Ullom<sup>3</sup> · L. R. Vale<sup>3</sup>

Received: 1 November 2021 / Accepted: 6 October 2022 / Published online: 9 November 2022  
© The Author(s), under exclusive licence to Springer Science+Business Media, LLC, part of Springer Nature 2022

### Abstract

The assessment of the absolute  $\nu$  mass scale is a crucial challenge in today's particle physics and cosmology. The only experimental method which can provide a model-independent measurement is the investigation of endpoint distortion in beta/electron capture spectra.  $^{163}\text{Ho}$  is a good choice thanks to its low electron capture Q value (about 2.8 keV), the proximity of the end-point to resonance M1 and its half-life (4570 years). The HOLMES experiment will exploit a calorimetric measurement of  $^{163}\text{Ho}$  decay spectrum deploying a large set of cryogenic micro-calorimeters containing implanted  $^{163}\text{Ho}$ . In order to get the best experimental sensitivity, it is crucial to combine high activity with very small undetected pileup contribution. Therefore, the main tasks of the experiment consist of: the development of about 1000 fast (3  $\mu\text{s}$  time resolution) cryogenic micro-calorimeters characterized by extraordinary energy resolution (down to few eV); the embedding of  $^{163}\text{Ho}$  source inside the calorimeters, avoiding to spoil detectors' thermodynamical properties (mainly heat capacity) and preventing pileup issues. Moreover, it is also necessary to avoid contamination from other radionuclides, mainly  $^{166m}\text{Ho}$ . Finally, an efficient high-bandwidth multiplexed readout has to be developed. The commissioning of the first implanted array is currently ongoing; the first data acquisition is expected to start in fall 2022. Here, the status of the experiment and the first results of detector commissioning will be discussed.

---

✉ M. De Gerone  
matteo.degerone@ge.infn.it

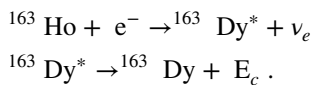
Extended author information available on the last page of the article

**Keywords** Neutrino mass measurement · Electron capture · Ho-163 · Transition-edge sensor

## 1 Introduction: The $^{163}\text{Ho}$ Electron Capture Decay

The neutrino mass measurement is one of the crucial topics in present-day particle physics. Among all the possible ways to estimate neutrino mass (cosmological considerations, neutrino-less double beta decay searches, direct measurements) a calorimetric measurement has the great advantage to rely only on kinematics considerations. Moreover, the usage of  $^{163}\text{Ho}$  for a calorimetric measurement avoids some sources of systematic errors related to the usage of an external source and decays into excited final states. An exhaustive review of these researches can be found in [1] and references therein.

$^{163}\text{Ho}$  decays via electron capture (EC) to an excited state of  $^{163}\text{Dy}$  [2]:



The  $^{163}\text{Dy}^*$  de-excitation energy  $E_c$  spectrum is then given by:

$$\begin{aligned}\frac{d\Lambda_{EC}}{dE_c} &= \frac{G_\beta^2}{4\pi^2} (Q - E_c) \sqrt{(Q - E_c)^2 - m_\nu^2} \\ &\times \sum_i K_i \frac{\Gamma_i}{2\pi} \frac{1}{(E_c - E_i)^2 + \Gamma_i^2/4}\end{aligned}\quad (1)$$

where  $G_\beta = G_F \cos \theta_c$  ( $G_F$  and  $\theta_c$  are the Fermi constant and the Cabibbo angle, respectively),  $m_\nu$  is the neutrino mass,  $\Gamma_i$  is the intrinsic width of the Breit-Wigner resonance centered at energy  $E_i$  and  $K_i$  includes all the factors related to nuclear processes [2]. Thus, the endpoint is shaped by the same phase factor as in  $\beta$  decay. A finite  $\nu$  mass would appear as a distortion of the spectrum in the region just below the end point which is shifted to  $(Q_{EC} - m_\nu)$ .  $^{163}\text{Ho}$  is considered to be a good candidate for this measurement for two reasons. Firstly, it has a very low  $Q$ -value ( $\sim 2.8$  keV [3]) close to the binding energy of the M1shell, which should enhance the number of events falling in the region of interest, since the  $m_\nu$  sensitivity roughly depends on  $1/(Q - E_{M1})^3$  [1]. Secondly, the short half-life of 4570 years allows for a reasonable constant activity with a “small” amount of atoms (1 Bq corresponding to  $2 \times 10^{11}$  atoms), making feasible the design of a detector-source system.

## 2 The HOLMES Experiment

The HOLMES collaboration aims to reach  $\mathcal{O}(\text{eV})$  sensitivity in a direct neutrino mass measurement taking advantage of the  $^{163}\text{Ho}$  EC decay described in Sect. 1. It is supposed to deploy a large number of Transition-Edge Sensors (TES) based cryogenic

microcalorimeters, arranged in arrays of 64 detectors, with each detector implanted with  $^{163}\text{Ho}$ . The goal is to reach the  $\mathcal{O}(\text{eV})$  sensitivity within few years of taking data. Cryogenic microcalorimeters have outstanding energy resolution, and the readout of a large number of channels by means of a multiplexed readout scheme has been already well established. A drawback of this kind of detector is the limited dynamic range. Therefore an optimized design is needed for each specific application. For this reason, a detailed Monte Carlo simulation has been developed [4] in order to evaluate the statistical sensitivity as a function of the detector performance, thus defining the needed energy and time resolution which in their turn define the final detector layout. Because one of the major drawbacks of the calorimetric technique is that all decays are collected inside the detector, the maximum activity is limited by the rate of accidental coincidences (pileup) and thus one of the main challenge of the experiment is to find a good compromise between the unresolved pileup fraction, the needed statistics and detector performance [5]. For the purpose of reaching the eV sensitivity, it will be necessary to measure at least  $3 \times 10^{13}$  decays with an energy resolution  $\Delta E \mathcal{O}(1\text{eV FWHM})$  and a time resolution  $\Delta t \sim 10\mu\text{s}$  (here time resolution is defined as capability to resolve piled-up events). Taking into account a 3 years of acquisition, an overall activity of about  $3 \times 10^5$  Bq corresponding to  $\sim 300$  Bq/detector is needed. Currently, we plan to proceed with a two-steps approach: first, to develop a single array made of 64 detectors that, with the above-mentioned activity should reach a 10 eV sensitivity in 1 month of measurement time and then move to the full scale (1000 detectors) experiment.

### 3 Holmium Production, Purification and Embedding System

One of the major challenges for HOLMES is the production and purification of  $^{163}\text{Ho}$  sample. This isotope doesn't exist in nature and thus has to be artificially produced. One way to obtain it is with neutron activation of an enriched  $^{162}\text{Er}$  compound ( $\text{Er}_2\text{O}_3$ ) in a nuclear reactor with the reaction:



$^{163}\text{Er}$  decays to  $^{163}\text{Ho}$  by electron capture with a half-life of 75 min. This is not the only relevant way of producing the  $^{163}\text{Ho}$  isotope [6], but it is the one with the higher production yield. Because of the large amount of impurities in the starting sample (different Er isotopes and other rare earth contaminations), this process leads to the production of many unwanted species together with  $^{163}\text{Ho}$  [7]. Amongst them, the most dangerous one is  $^{166m}\text{Ho}$ , which has a long half life (1200 years) decay to  $^{166}\text{Er}$ , with the emission of a large number of gamma-rays between 80 and 1400 keV [8]. Moreover,  $\mathcal{O}(\text{GBq})$  of  $^{170}\text{Tm}$  and  $^{171}\text{Tm}$  are expected to be produced. Those isotopes have half-lives of 128 days and 2 years respectively. Thus they represent the most significant risk for handling the irradiated sample material. Therefore, a two-fold purification process to isolate  $^{163}\text{Ho}$  is needed: radiochemical purification to remove everything but Ho and mass separation to get rid of  $^{166m}\text{Ho}$ . The first step is done at Paul Scherrer Institute via a sophisticated chemical separation based on ion exchange chromatography [7]. This process has been shown to be highly efficient

( $\epsilon > 98.6\%$ ) on a 20 mg  $\text{Er}_2\text{O}_3$  irradiated sample. Moreover, at the end of the procedure more than 90% of non-activated  $^{162}\text{Er}$  can be recovered and irradiated again. 3 different  $\text{Er}_2\text{O}_3$  batches have been irradiated and purified, for a total resulting  $^{163}\text{Ho}$  activity of about 110 MBq. One more sample was recently irradiated and will be soon purified, resulting in an additional 80 MBq (estimation coming from previously measured yields). Currently, the total available amount of  $^{163}\text{Ho}$  is estimated to be sufficient to fulfill HOLMES' requirement.

The second step of sample purification relies on magnetic dipole mass separation and will take place in Genoa's laboratory, where a specially designed ion implanter has been recently installed and commissioned [9]. A scheme of the machine layout is shown in Fig. 1. The implanter consists of an argon-fed sputtering ion source with maximum accelerating voltage of 50 kV, a dipole magnet able to reach field intensities up to 1.1 T, some diagnostic tools, an electrostatic triplet, a X-Y steering magnet and a target chamber. The electrostatic triplet, the X-Y steering magnet and the target chamber are currently not yet installed. The machine has the two-fold purpose of performing a mass selection of the beam, thus giving a possibility to remove any mass other than 163 u from the target region allowing an implantation of the Ho ions into a gold substrate, with an expected implantation depth of  $\varnothing$  (20 nm) for 25 keV ions (evaluated on SRIM simulation [10]). The target chamber is specially designed in such a way to permit a gold layer deposit by sputter process during Ho implantation. This is needed because the maximum Ho concentration is expected to saturate after few Bq. At the end of the process a final layer of 1  $\mu\text{m}$  of gold is needed to complete the calorimeter absorber, obtaining a full encapsulation of the Ho source.

The beam is generated by a Penning-sputter-based ion source. The beam is generated starting from a sputter target which contains Ho in different chemical forms (typically a  $\text{H}(\text{NO}_3)_3$  solution). Currently, different techniques to prepare the target are under investigation. Among them, the most promising one seems to be the production of a sintered matrix made by a mixture of metal powders (Ti, Ni, Sn and Ho in different proportions) in which Ho solution can be added. The choice of materials was driven by the need to have a sinter with good mechanical properties. More details about sputter target production can be found in [9].

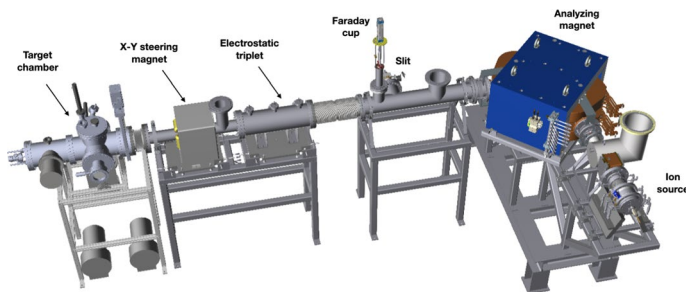


**Fig. 1** (Color online) Scheme of the ion implanter. See text for details

## 4 Detector Design and Production

The detectors employed by HOLMES will be a set of Transition Edge Sensor (TES) based microcalorimeters. The TES will be a  $125 \times 125 \mu\text{m}^2$  Mo/Cu bi-layer sensor placed on a  $500 \text{ nm SiN}_x$  suspended membrane. The bi-layer thickness is adjusted to have a critical temperature around  $100 \text{ mK}$ . The absorber consists of a  $200 \times 200 \times 2 \mu\text{m}^3$  of gold, which should be able to fully contain the 99.99% of the 2-keV electrons and 96.73% of the 2-keV photons produced in  $^{163}\text{Ho}$  decay. The effect of the fraction of non-detected events has been extensively simulated with MonteCarlo simulations. Due to the need to fully encapsulate the Ho ions inside the absorber, the detectors undergo a multi-step fabrication procedure, which is shown schematically in Fig. 2a. The first step is done at the National Institute for Standards and Technology (NIST, Boulder, Co, USA) where the microcalorimeters are fabricated up to the deposition of a  $1 \mu\text{m}$  Au layer of the calorimeter absorber. Then, the devices undergo the ion implantation / gold co-evaporation processes. A total activity of the order of  $300 \text{ Bq}$  is expected to be embedded inside the detector. Ultimately, the devices are completed with an additional  $1 \mu\text{m}$  Au layer, which guarantees the containment of the deposited radiation. The very last step consists of the release of the  $\text{SiN}_x$  membrane. The usage of membrane-suspended detectors prevents phonons escaping into the silicon substrate. Membrane release could be done in two ways: a Deep Reactive Ion Etching (DRIE) process or a KOH-based wet etching. Both processes are now under test in order to choose the best performing one. A picture of a detector is showed in Fig. 2b.

The detectors are grouped in arrays, each one containing 64 devices (see Fig. 2c). The array's layout is optimized in order to get the best geometric factor efficiency

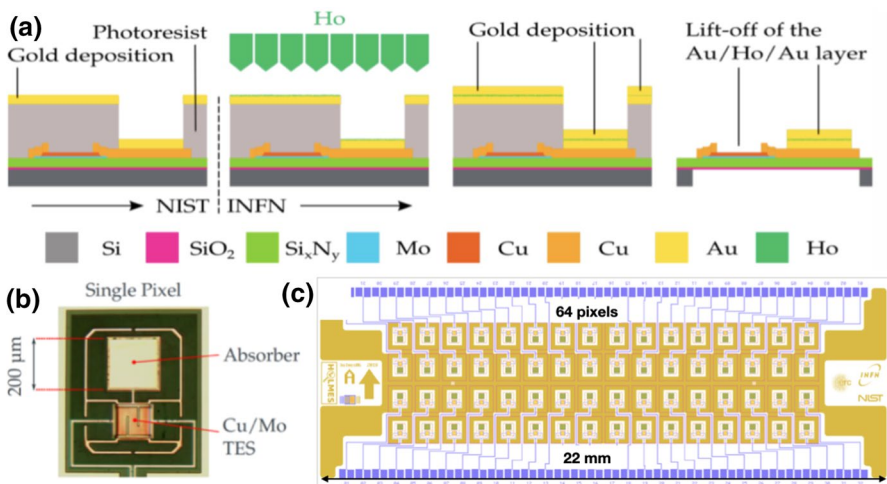


**Fig. 2** (Color online) **a** schematic of the  $\mu$ -calorimeter production process. The arrays is produced firstly up to the deposition of the first layer of gold. Then Ho is implanted and encapsulated with an additional  $1 \mu\text{m}$  gold layer. Lift off process and membrane release completed the detector production. **b** picture of a real detector **c** schematic of the final 64 detectors array layout

(currently estimated to be around  $1.2 \times 10^{-2}$ ) for the implantation process, taking into account the beam size (expected to be around 2.5 mm FWHM). Moreover, the chosen design also minimizes crosstalk and stray inductance.

## 5 Multiplexed DAQ and Detectors Test

The HOLMES readout is based on the microwave multiplexing system ( $\mu$ -MUX) [11] designed and developed by NIST. The readout scheme is shown in Fig. 3, for both single- (Fig. 3a) and multi-channel (Fig. 3b) readout.

According to this scheme, each DC-biased TES is coupled to a dissipationless radio-frequency (RF) SQUID which in its turn is coupled to a superconducting  $\lambda/4$ -wave resonators in the GHz range. In addition, a flux-ramp modulation is applied to the SQUID to linearize the response [12]. Thus, a change in TES current induces a change in the RF-SQUID input flux which corresponds to a change in the resonance frequency and phase of the superconducting resonator. In this way, it is straightforward to multiplex many RF carriers by tuning the resonators at different frequencies. The microwave multiplexing technique is the most suitable system for HOLMES, since it provides a larger bandwidth (2 MHz) for the same number of multiplexed detectors. The  $\mu$ -MUX system is suitable for a fully digital approach based on the Software Defined Radio (SDR) technique: a comb of frequency carriers are generated by digital synthesis in the MHz range (0–512 MHz) and up-converted by mixing them with a signal in the GHz range (4–8 GHz, RF band). The GHz comb is sent to the cold  $\mu$ -MUX chips coupled to the detectors and is then amplified by a low temperature and low noise High Electron Mobility Transistor (HEMT). Finally, it is sent back to room temperature. The output signal is down-converted and individual channel signal recovery is performed by software on the digitized signal. In its final configuration HOLMES will implement an SDR multiplexed readout exploiting the Reconfigurable Open Architecture Computing Hardware (ROACH2 [13]) board. The full chain system is made by a digital signal processing board (ROACH2), a DAC (for comb generation) and ADC (512 MS/s, 12 bit, 2 channels) boards, a board for signal up- and down-conversion, and optically decoupled interfaces for fast data transfer.

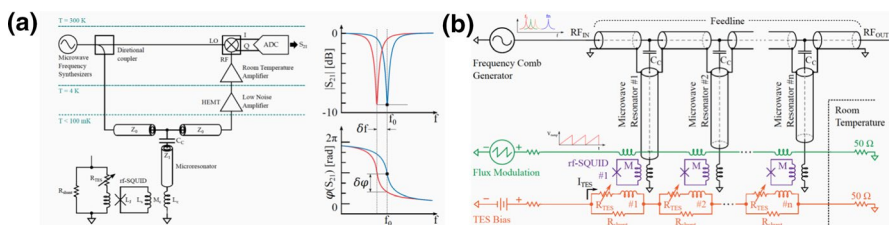
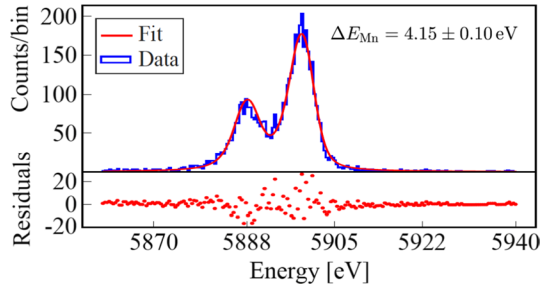


**Fig. 3** (Color online) Multiplexing of TES sensor. **a** concept for one multiplexed channel. **b** scheme for multiplexing readout of a TES array

**Fig. 4** (Color online)  $^{55}\text{Fe}$  lines measured with HOLMES' microcalorimeter



In order to test the full HOLMES fabrication chain from the detector to the readout scheme, several sub-arrays were produced following each step except the implantation process. In this case, the membrane release was done by means of KOH wet etching. The detectors were excited with an X-ray fluorescence source, based on a primary  $^{55}\text{Fe}$  source which illuminates targets of various materials. Signals were recorded using the final HOLMES DAQ chain described in this section. The result obtained on the best performing detector is shown in Fig. 4: an energy resolution of  $(4.15 \pm 0.10)\text{eV}$  evaluated on the Mn  $K_{\alpha}$  lines has been demonstrated [14]. The spectral lines were fitted with a set of Lorentzian functions convoluted with a gaussian one. The fitted value is perfectly compatible with a required resolution of few eV. The pulse rise time has been measured to be around  $20 \mu\text{s}$ , while the decay time was found to be  $\sim 300\mu\text{s}$ . Both values are slightly higher than expected design ones (about  $10 \mu\text{s}$  and  $200 \mu\text{s}$ , respectively), but still match HOLMES' requirements.

## 6 Conclusion and Prospects

The development and the commissioning of the setup of the HOLMES experiment are almost completed. Currently, a first set of detectors has already been deployed, following the full fabrication procedure, with the only exception of Ho implantation. Moreover, those detectors have been measured under radiation produced by different sources ( $^{55}\text{Fe}$  source pointing a mixture of  $\text{NaCl}$  and  $\text{CaCO}_3$ ) in the range of 1-5 keV. The best performing detector showed an energy resolution of  $(4.15 \pm 0.10) \text{ eV}$  evaluated on the Mn  $K_{\alpha}$  lines. The production of a first set of  $^{163}\text{Ho}$  implanted detectors is supposed to be completed by the end of the year 2022.

**Acknowledgements** This work was supported by the European Research Council (FP7/2007-2013), under Grant Agreement HOLMES No. 340321, and by the INFN Astroparticle Physics Commission 2 (CSN2). We also acknowledge the support from the NIST Innovations in Measurement Science program for the TES detector development.

## Declarations

**Conflict of interest** The data supporting the findings of this study are available from the authors on request.




## References

1. A. Nucciotti, Adv. High Energy Phys. **2016**, 9153024 (2016)
2. A. De Rujula, M. Lusignoli, Phys. Lett. B **118**, 429 (1982)
3. S. Eliseev et al., Phys. Rev. Lett. **115**, 062501 (2015)
4. A. Nucciotti et al., HOLMES collaboration. Eur. Phys. J. C **75**, 112 (2015)
5. M. Borghesi et al., Eur. Phys. J. C **81**, 385 (2021)
6. O. Kawakami et al., Phys Rev C. **38**(4), 1857–60 (1988)
7. S. Heinitz et al., PLoS one **13**(8), e0200910 (2018)
8. [http://www.nucleide.org/DDEP\\_WG/Nuclides/Ho-166m\\_tables.pdf](http://www.nucleide.org/DDEP_WG/Nuclides/Ho-166m_tables.pdf)
9. M. De Gerone et al. J. Low Temp. Phys. This Special Issue (2021)
10. <http://www.srim.org/>
11. J.A.B. Mates et al., Appl. Phys. Lett. **92**(2), 023514 (2008)
12. J.A.B. Mates et al., J. Low Temp. Phys. **167**(5), 707 (2012)
13. S. McHugh et al., Rev. Sci. Instrum. **83**, 044702 (2012)
14. A. Giachero et al., IEEE Trans. Appl. Supercond. **31**, 5 (2021)

**Publisher's Note** Springer Nature remains neutral with regard to jurisdictional claims in published maps and institutional affiliations.

Springer Nature or its licensor (e.g. a society or other partner) holds exclusive rights to this article under a publishing agreement with the author(s) or other rightsholder(s); author self-archiving of the accepted manuscript version of this article is solely governed by the terms of such publishing agreement and applicable law.

## Authors and Affiliations

M. De Gerone<sup>1</sup>  · B. Alpert<sup>3</sup> · M. Balata<sup>4</sup> · D. T. Becker<sup>3</sup> · D. A. Bennett<sup>3</sup> · A. Bevilacqua<sup>1</sup> · M. Borghesi<sup>5,6</sup> · G. Ceruti<sup>5</sup> · G. De Bodin De Galebent<sup>7</sup> · R. Dressler<sup>7</sup> · M. Faverzani<sup>5,6</sup> · M. Fedkevych<sup>1,2</sup> · E. Ferri<sup>5</sup> · J. W. Fowler<sup>3</sup> · G. Gallucci<sup>1</sup> · J. D. Gard<sup>3</sup> · F. Gatti<sup>1,2</sup> · A. Giachero<sup>5,6</sup> · G. C. Hilton<sup>3</sup> · U. Köster<sup>8</sup> · M. Lusignoli<sup>9</sup> · P. Manfrinetti<sup>10</sup> · J. A. B. Mates<sup>3</sup> · E. Maugeri<sup>7</sup> · S. Nisi<sup>4</sup> · A. Nucciotti<sup>5,6</sup> · L. Parodi<sup>1</sup> · G. Pessina<sup>5,6</sup> · S. Ragazzi<sup>5,6</sup> · C. D. Reintsema<sup>3</sup> · D. R. Schmidt<sup>3</sup> · D. Schumann<sup>7</sup> · F. Siccardi<sup>1</sup> · D. S. Swetz<sup>3</sup> · J. N. Ullom<sup>3</sup> · L. R. Vale<sup>3</sup>

<sup>1</sup> Istituto Nazionale di Fisica Nucleare (INFN), Genoa, Italy

<sup>2</sup> Department of Physics, University of Genoa, Genoa, Italy

<sup>3</sup> National Institute of Standards and Technology (NIST), Boulder, CO, USA

<sup>4</sup> Laboratori Nazionali del Gran Sasso (LNGS) INFN, Assergi, Italy

<sup>5</sup> Istituto Nazionale di Fisica Nucleare (INFN), Milan-Bicocca, Italy

<sup>6</sup> Department of Physics, University of Milan-Bicocca, Milan, Italy

<sup>7</sup> Paul Scherrer Institute (PSI), Villigen 5303, Switzerland

<sup>8</sup> Institut Laue-Langevin (ILL), Grenoble, France

<sup>9</sup> Istituto Nazionale di Fisica Nucleare (INFN), Rome, Italy

<sup>10</sup> Department of Chemistry, University of Genoa, Genoa, Italy